THE ASTROPHYSICAL JOURNAL, 313:378–388, 1987 February 1


# DISCOVERY OF FAST-MOVING NITROGEN-RICH EJECTA IN THE SUPERNOVA REMNANT CASSIOPEIA A[1]

ROBERT A. FESEN[2]
Center for Astrophysics and Space Astronomy, University of Colorado
ROBERT H. BECKER
Department of Physics, University of California at Davis; and Institute of Geophysics and Planetary Physics, Lawrence Livermore National Laboratory
AND
WILLIAM P. BLAIR[2]
Department of Physics and Astronomy, The Johns Hopkins University
*Received 1986 June 2; accepted 1986 July 30*

## ABSTRACT

Deep interference-filter CCD images of regions along the periphery of Cas A reveal the presence of several additional emission knots and extended diffuse nebulosity to the east and southwest of the remnant and well outside Cas A's main optical and radio shell. Comparisons with earlier published photographs indicate that five of these outlying knots exhibit large proper motions ($\mu = 0\farcs50$–$0\farcs65$ yr$^{-1}$) comparable to those seen for the highest velocity "fast-moving knots" found in the remnant's northeastern "jet." Spectra of these knots show radial velocities ranging from +400 to −2200 km s$^{-1}$. While possessing kinematic properties like those of the remnant's oxygen- and sulfur-rich ejecta, these new features show only strong emission lines of H$\alpha$ and [N II] with relative line intensities similar to those seen in the low-velocity and nitrogen-rich "quasi-stationary flocculi." Spectra of the diffuse nebulosity just east of the remnant indicates a low radial velocity and emission line intensities indicative of either a low-ionization H II region or a shock-heated gas.

The detection of fast-moving nitrogen-rich knots represents the discovery of a new class of Cas A ejecta which we interpret as fragments from the progenitor's photospheric layers at the moment of supernova outburst. This implies a probable late WN spectroscopic classification (i.e., WN7–WN9) for the Cas A progenitor star. Furthermore, the position of these knots outside the remnant's main shell but at radial distances less than that seen for the northeast "jet" indicates both a larger remnant structure than previously believed and a nonuniform expansion. We discuss the observed properties of the detected outlying emission and its implications for understanding Cas A and Type II supernovae and supernova remnants in general.

*Subject headings:* nebulae: individual — nebulae: supernova remnants — stars: supernovae

## I. INTRODUCTION

The radio source Cassiopeia A is believed to be a young Galactic supernova remnant (SNR) resulting from an unreported supernova which occurred during the latter half of the 17th century. Although a strong source at both radio and X-ray wavelengths, this remnant is fairly faint optically; it consists of over 100 emission-line knots and small filaments organized into an incomplete shell structure of radius 2′. At an assumed distance of 2.8 kpc (van den Bergh 1971*b*), this corresponds to a linear radius for the remnant of 1.6 pc.

Spectroscopic and proper motion studies of Cas A's optical filaments made over several decades (Baade and Minkowski 1954; Minkowski 1957, 1959, 1968; van den Bergh and Dodd 1970; van den Bergh 1971*b*; Peimbert and van den Bergh 1971; Peimbert 1971; Kamper and van den Bergh 1976; Kirshner and Chevalier 1977; Chevalier and Kirshner 1978, 1979; van den Bergh and Kamper 1983, 1985) have categorized the remnant's optical nebulosity into two distinct components. (1) About 120 so-called "fast-moving knots" (FMKs) which exhibit large proper motions ($\mu = 0\farcs2$–$0\farcs7$ yr$^{-1}$) and high radial velocities (up to 5500 km s$^{-1}$), implying space velocities in the range of 4000–9500 km s$^{-1}$. These knots show strong lines of oxygen, sulfur, and argon with no detectable hydrogen or helium and thus are thought to represent undiluted ejecta from the disrupted core of a massive star (Lamb 1978; Chevalier 1979). (2) Nearly three dozen "quasi-stationary flocculi" (QSFs), which have much lower proper motions ($\mu < 0\farcs03$ yr$^{-1}$) and radial velocities ($0 < V_r < -450$ km s$^{-1}$), indicative of an expansion age of ~11,000 yr, considerably longer than the ~300 yr age estimated for the remnant. The QSFs exhibit relatively strong lines of nitrogen and helium compared to H$\alpha$, suggesting substantial CNO enrichment, and are believed to constitute circumstellar material lost by the progenitor star prior to the supernova (SN) outburst.

While Cas A's X-ray and radio morphology is generally similar to the incomplete shell seen in the optical, some differences are observed for the remnant's outermost features. A northeastern "flare" or "jet" of ejecta which extends out to a radial distance almost double that of the main shell (i.e., ~4′) is more prominently seen in the optical than in radio or X-ray maps. This northeast jet appears composed of sulfur-rich FMKs having the largest proper motions seen in the remnant. Also outside the main shell are five very faint apparent QSFs located ~2′.5 to the south-southwest discovered by van den

[1] Based in part on research done at Lick Observatory, University of California.

[2] Visiting Astronomer, Kitt Peak National Observatory, National Optical Astronomy Observatories, operated by the Association of Universities for Research in Astronomy, Inc., under contract with the National Science Foundation.

Bergh and Kamper (1983). One of these QSFs may have coincident radio emission (Bell 1977). However, these QSFs as well as the northeast jet lie well within a reported faint 6′ radius X-ray halo which may surround the entire remnant (Stewart, Fabian, and Seward 1983). Finally, there is a very faint and patchy optical H II region detected in the local vicinity of Cas A (Minkowski 1968; van den Bergh 1971*b*).

In this paper, we report the discovery of a new type of Cas A filament that possesses some characteristics of both the FMKs and the QSFs. That is, they show large proper motions and radial velocities like the FMKs yet have hydrogen emission and evidence of appreciable nitrogen enrichment like the QSFs. These new emission features are located outside the remnant's main shell and appear likely to be fragments from the surface layers of the progenitor star. They therefore provide important clues as to the nature and spectral classification of the Cas A progenitor star at the time of supernova outburst. We also report the detection of additional QSFs to the south-southwest as well as considerable diffuse emission along two sections of the remnant's periphery. The observational data and results are described in §§ II and III, with the implications regarding the remnant and progenitor star discussed in § IV.

## II. OBSERVATIONS

### *a) Imaging*

Deep optical images of several regions just outside Cas A's main optical and radio shell (see Fig. 1 [Pl. 2]) were obtained on 1985 July 22 using the Cassegrain CCD detector on the 3 m Shane telescope at Lick Observatory. This device uses a Texas Instruments 800 × 800 pixel CCD for both spectroscopic and image data collection (Miller 1983). For imaging, only the central 200 × 200 pixels were utilized, producing a field of view of about 2.′5 × 2.′5 with a pixel size of 0.″73. This spatial resolution is less than the seeing on this night, which was between 1″ and 2″. Images were obtained using several narrow passband interference filters. These included an Hα + [N II] filter having $\lambda_0 = 6576$ Å (FWHM = 104 Å) and a maximum transmission of 60%, and a red continuum filter with $\lambda_0 = 7030$ Å (FWHM = 274 Å) and a peak transmission of 90%. These two filters provided effective "on" and "off" passband images for easy identification of Hα + [N II] emission features. Typical exposure integration was 300 s in order to prevent excessive charge "bleeding" from bright stars (< 16 mag) in the field of view.

Image processing involved bias background subtraction and dome flat-field corrections. Distortion corrections were not applied to the data, since distortion constants for the Shane telescope Cassegrain CCD camera are not known. Unfortunately, flat-field calibration images did not always provide very accurate flat field–corrected images, resulting in background nonuniformities, especially near the images' edges. Nonetheless, individual exposures of just 300 s revealed several previously undetected faint emission features. The limiting detected Hα flux for these images is $\sim 23.5$ mag arcsec$^{-2}$, corresponding to an emission measure of $\sim 25$ cm$^{-6}$ pc.

Proper motion estimates were obtained for several detected emission features where positional displacements were suspected from examinations of earlier epoch photographs (see Table 1). These estimates were determined through direct comparisons of our CCD images with identical scale reproductions of a deeply exposed 1976 5 m telescope plate with the resultant measurements reduced to the coordinate system of Kamper and van den Bergh (1976). This method was considered adequate to yield the desired initial proper motion estimates (i.e., ±0.″1 yr$^{-1}$), particularly in view of the often exceedingly weak detection of the features on earlier photographs, a time interval of only 9 yr, and the difficulty of producing precision measurements using data from different image media.

TABLE 1

PROPER MOTIONS FOR FAST-MOVING FLOCCULI

| FMF | Radial Distance (1976) | Radial Proper Motion (yr$^{-1}$) | Transverse Velocity[a] (km s$^{-1}$) | $T_0$ (yr) |
|---|---|---|---|---|
| 1[b] | 192″ | 0.″65 ± 0.″10 | 8600 | 1681 |
| 2 | (182)[c] | ... | ... | ... |
| 3 | 171 | 0.56 ± 0.10 | 7400 | 1671 |
| 4 | 144 | 0.50 ± 0.10 | 6600 | 1688 |
| 5 | 154 | 0.51 ± 0.05[d] | 6800 | 1674 |
| 6 | 155 | 0.51 ± 0.10 | 6800 | 1672 |
| 7 | (163)[c] | ... | ... | ... |
| 8 | 184 | ~0.60 | ~8000 | ~1670 |
| 9 | (175) | 0.58 ± 0.10[d] | 7700 | 1674 |
| (SE)[e] | 172 | ... | ... | ... |
| Main shell[f] | 100 | 0.31 | 4100 | 1653 |
| Northeast jet[f] | 180 | 0.60 | 8000 | 1671 |

[a] Assuming a distance of 2.8 kpc.
[b] FMF 1 = R39.
[c] Estimated for 1976.
[d] Also using position on 1958 Aug 11 plate (see van den Bergh and Dodd 1970).
[e] Suspected FMF in the southeast (see Fig. 10).
[f] Average values from Kamper and van den Bergh 1976.

### *b) Spectroscopy*

Follow-up spectroscopy of some of the emission features discovered on the Lick images was obtained on 1985 September 18 and October 19 with the cryogenic CCD camera attached to the KPNO 4 m telescope. This instrument consists of a collimator lens, grism, and a liquid nitrogen–cooled Texas Instruments 800 × 800 pixel CCD. A 300 grooves mm$^{-1}$ grism (No. 770) was used together with an order-separating filter (GG 420) to provide a wavelength coverage of 4600–8000 Å with 12–15 Å spectral resolution. On September 18, a spectrum of the extended diffuse nebulosity located due east of the remnant was obtained using a 3.″2 × 4.′5 long slit rotated to a position angle of 150°. Integration time was 3000 s, with the seeing at 1″–2″. Spectra of some of the faint emission knots located south-southwest of Cas A were obtained on October 19 also, using a 3000 s integration and a 2.″5 × 4.′5 slit at a position angle of 30°.

Data reduction was performed using Kitt Peak reduction software for the cryogenic camera data taken in long-slit mode. This procedure included bias subtraction, removal of pixel-to-pixel sensitivity variations, wavelength calibrations, atmospheric extinction corrections, and calibrations for slit and instrumental spectral response functions. The spectral response of the spectrograph was calibrated through observations of standard stars (Oke 1974) observed at several positions along the slit to compensate for response variations across the CCD chip. Sky subtraction was accomplished by averaging two strips of apparent blank sky areas on either side of observed emission features.

Measured line strengths relative to Hα are given in Table 2, listed under $F(\lambda)$. For the extended eastern diffuse region and knot 7, line intensities have been corrected for interstellar

PLATE 2

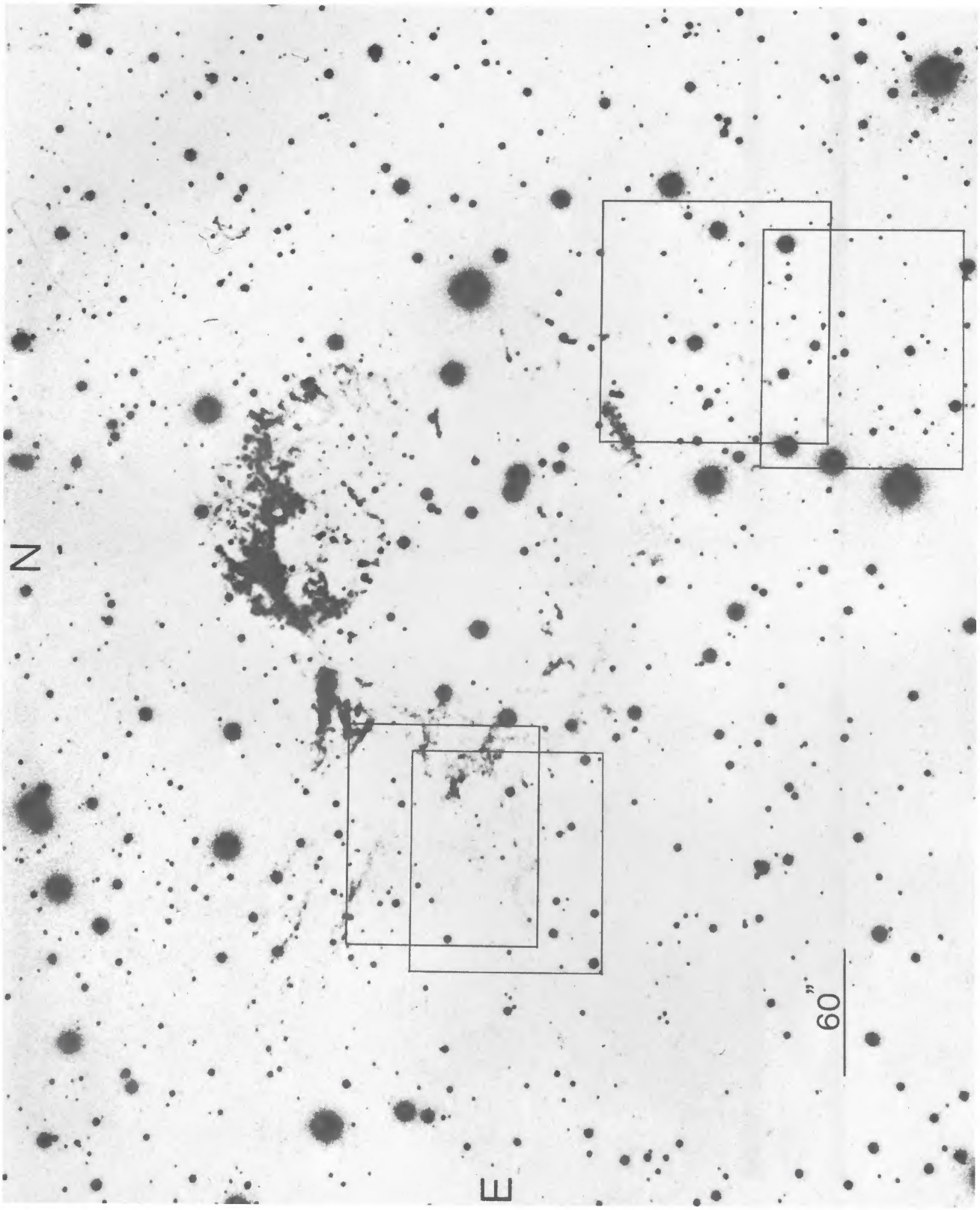


FIG. 1.—Broad-band red 1976 July 2 Hale Observatory 5 m plate of the supernova remnant Cas A. The four regions for which deep CCD imaging was obtained are indicated. (Photograph courtesy of S. van den Bergh.)

TABLE 2

RELATIVE LINE INTENSITIES AND RADIAL VELOCITIES

($H\alpha = 1.00$; $A_v = 4.3$)

| LINE | $\lambda$ (Å) | DIF. NEB.[a] | | KNOT 7 | | FMF 1 | FMF 2 | FMF 3 | R38 | 1Q1[b] |
|---|---|---|---|---|---|---|---|---|---|---|
| | | $F(\lambda)$ | $I(\lambda)$ | $F(\lambda)$ | $I(\lambda)$ | $F(\lambda)$ | $F(\lambda)$ | $F(\lambda)$ | $F(\lambda)$ | $F(\lambda)$ |
| Hβ | 4861 | (0.05) | (0.27) | (0.05) | (0.27) | ... | ... | ... | ... | 0.03 |
| [O III] | 5007 | 0.20 | 0.85 | 0.17 | 0.72 | ... | ... | ... | ... | 0.02 |
| [O I] | 6300 | <0.15 | <0.20 | <0.10 | <0.15 | <0.7 | ... | ... | ... | 0.21 |
| [N II] | 6548 | ... | ... | ... | ... | 1.3 | (1.0) | 0.9 | (0.6) | 0.83 |
| Hα | 6563 | 1.00 | 1.00 | 1.00 | 1.00 | 1.0 | 1.0 | 1.0 | 1.0 | 1.00 |
| [N II] | 6583 | 0.51 | 0.51 | 0.49 | 0.49 | 4.1 | 2.9 | 2.8 | 1.5 | 2.52 |
| [S II] | 6725 | 0.50 | 0.46 | 0.42 | 0.39 | <0.5 | <0.5 | <0.5 | <0.5 | 0.07 |
| [Fe II] | 7155 | (0.06) | (0.06) | (0.04) | (0.04) | ... | ... | ... | ... | ... |
| [O II] | 7325 | ... | ... | (0.06) | (0.06) | ... | ... | ... | ... | 0.15 |
| $V_r$ (km s$^{-1}$) | ... | −30 | | −60[c] | | −425 | −2150 | −2175 | −40 | +41 |

NOTE.—Parentheses indicates significantly more uncertain values.

[a] Diffuse emission region north of Knot 7.

[b] From Kirshner and Chevalier 1977.

[c] High-velocity [N II] emission is present at $V_r = +400$ km s$^{-1}$ (= FMF 7).

reddening, assuming $A_v = 4.3$ (Searle 1971), and are listed under $I(\lambda)$. The approximate observed flux for knot 7 is $1 \times 10^{-14}$ ergs cm$^{-2}$ s$^{-1}$. The estimated error in the observed relative line strengths for the brighter emission lines is ±25%. Radial velocity measurements are estimated to be accurate to ±75 km s$^{-1}$ (with the exception of fast-moving flocculus [FMF] 2 and R38, which are known to ±125 km s$^{-1}$) and are listed converted to heliocentric values.

## III. RESULTS

Deep CCD interference-filter images were obtained for four target fields outside Cas A's main shell (see Fig. 1). These images were taken in order to explore the possibility of additional QSFs southwest of the remnant besides the five already reported by van den Bergh and Kamper (1983) and to investigate the extent of the faint diffuse emission adjacent to the remnant's eastern rim. Despite short integration times, the resultant images yielded detection of substantially weaker emission features than are visible on most previously published images of the remnant. Use of a narrow-passband Hα + [N II] filter produced effective sky background reduction while limiting detection to only Hα + [N II] emission features like QSFs and avoiding FMK–type emission. Moreover, the use of continuum image subtraction provided nearly unambiguous line-emission feature identification.

Our Hα + [N II] image of the region immediately to the remnant's southwest is shown in Figure 2 (Plate 3). As can be seen more readily in the continuum-subtracted display of the image presented in the lower panel, numerous emission knots and nebulosity (visible as dark areas) are present in this region. The northernmost emissions visible, R9, R20, and R22 (using the nomenclature of Kamper and van den Bergh 1976 and van den Bergh and Kamper 1985) lie along the main shell's southwestern rim. The white area to the extreme upper left of the image lying between R9 and R22 is due to a FMK (KB 40) detected via its [Ar III] λ7136 emission on the "continuum" image. Further to the south-southwest, and consequently lying well outside the main optical and radio shell, are four of the five outlying QSFs (R37–R40) identified by van den Bergh and Kamper (1983). In contrast to the earlier weak detection of these knots, our images shows appreciable emission and associated structure. Although the two knots comprising R37 (n and s) appear virtually stellar on our image, R38 appears quite extended, having a crescent-like shape with fainter diffuse emission extending to the north and west. In addition to these four QSFs, several additional emission features can be seen, most of which have not been detected previously. These new features appear concentrated along a nearly unbroken line of emission extending southward from R20 through R38 and continuing down to the images's southern edge at R39 and R40. Much of this very faint emission appears filamentary or diffuse in structure and seemingly either associated with a QSF or connecting two knots together.

Van den Bergh and Kamper (1985) determined proper motions for four of the five previously known outlying QSFs and found them to exhibit similar motions to QSFs located closer to the remnant's center. A proper motion estimate for the remaining one, R39, could not be determined, it having apparently faded sufficiently to prevent its detection on their 1983 plates. However, a comparison of our 1985 image to their 1976 photograph revealed R39, though at a substantial southwestern displacement from its 1976 position (see Fig. 3 [Pl. 4]). The observed shift of nearly 6″ implies a proper motion during the intervening 9 yr of 0.″65 ± 0.″10 yr$^{-1}$ in a direction away from Cas A's expansion center (see Table 1). An alternate explanation involving the near-simultaneous brightening and fading of two independent knots is unlikely, especially in view of observed large radial velocities (see below). This conclusion is also supported by the existence of a similar but somewhat smaller proper motion of 0.″56 ± 0.″10 yr$^{-1}$ for a fainter and previously unidentified emission feature (No. 3; Fig. 3) positioned some 20″ northeast of R39 (No. 1).

In order to resolve the nature of these high proper motion "QSF–like" emission features, a 4.′5 long slit was placed so as to intercept both features (1 and 3) as well as a fainter diffuse knot (No. 2) located in between (see Fig. 4). This slit arrangement also crossed over the very faint eastern diffuse edge of R38. The resultant spectrum, shown in Figure 4, shows that features 1–3 possess strong Hα and [N II] λλ6548, 6583 emission like that seen for R38 and other QSFs (van den Bergh 1971*b*). Observed relative line intensities are listed in Table 2. No emission lines due to [O I], [O II], [O III], or [S II] were detected, as is typically the case for FMKs (see the FMK spectrum also shown). Also, no emission was detected farther to the

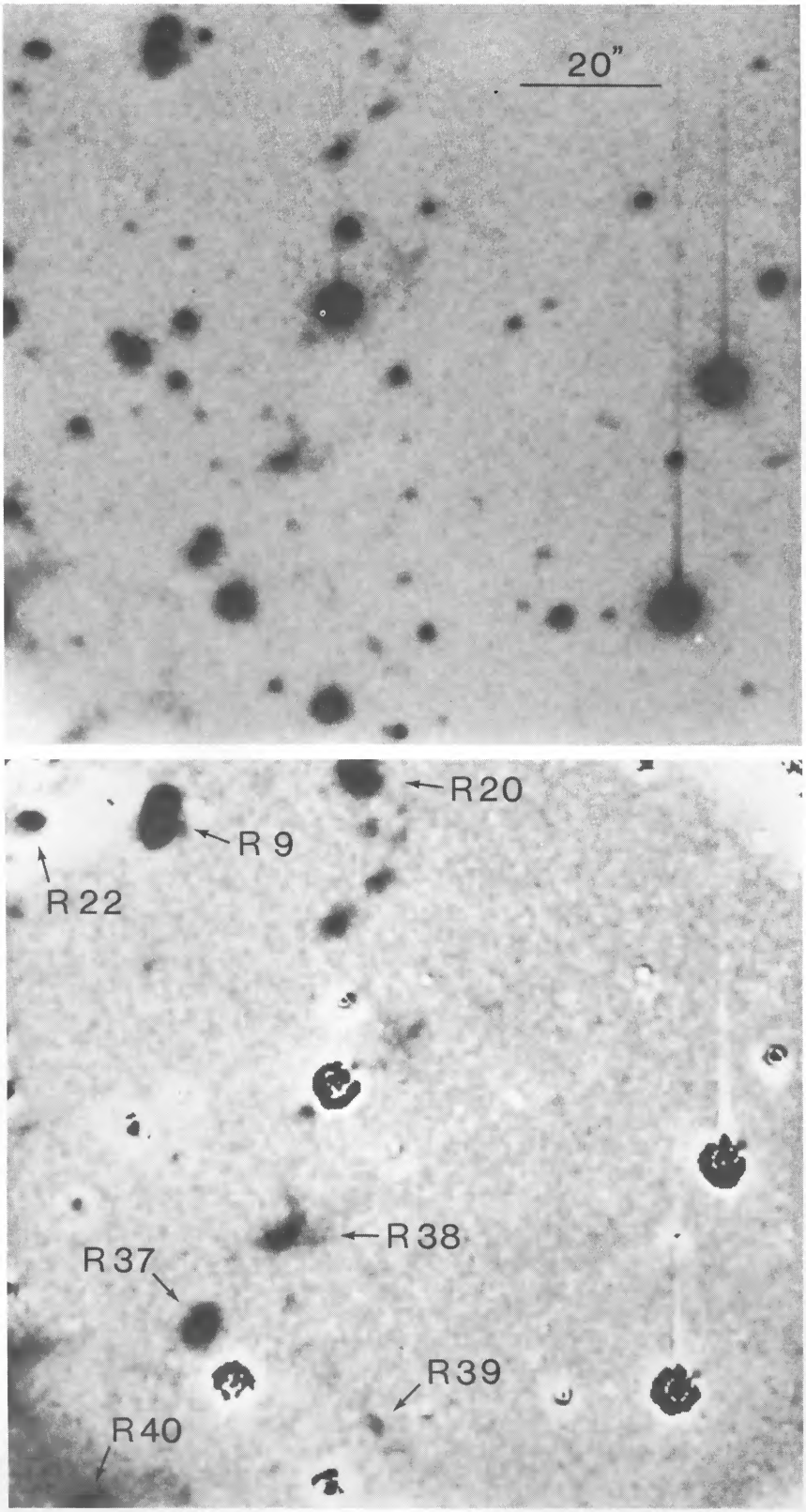


FIG. 2.—(*top*) Hα + [N II] CCD image of the region immediately south-southwest of the remnant showing the presence of several outlying QSFs. (*bottom*) Red continuum-subtracted Hα + [N II] display, enhancing the visibility of detected line-emission features (note: incomplete bright star subtraction is due to mismatch of filter passbands). An almost continuous line of emission extends from the remnant's southwestern rim (R20) to nearly 2′ south at R39 and R40. North is at top, east to the left.

FESEN, BECKER, AND BLAIR (*see* page 380)

PLATE 4

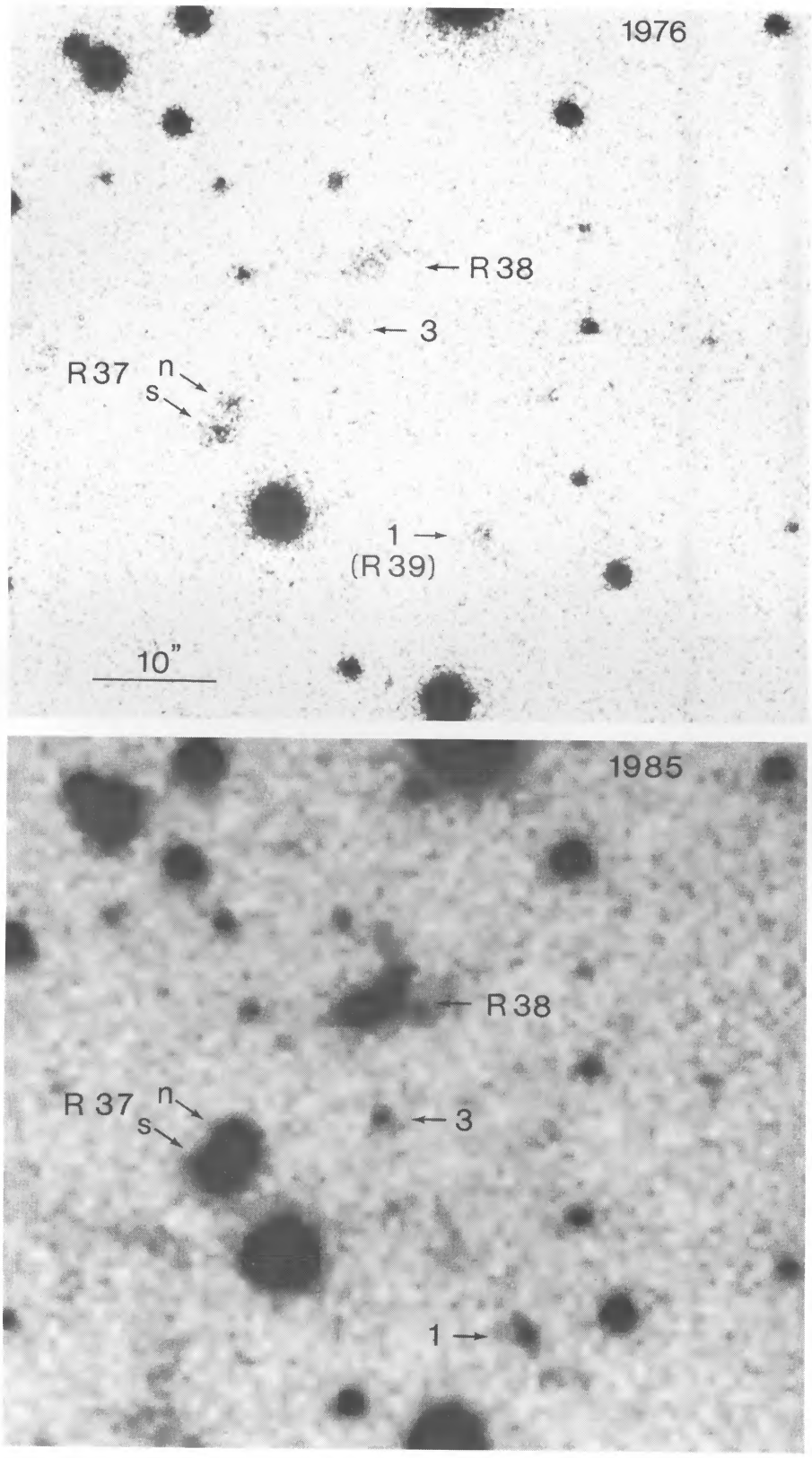


FIG. 3.—Enlargements of the south-southwest region. (*top*) Broad passband red 1976 photograph showing three of five previous known QSFs (R37–R39) which lie outside Cas A's main optical and radio shell. (*bottom*) 1985 CCD Hα + [N II] image of same region. Note the displacement of features No. 1 (= R39) and No. 3 to the southwest and away from remnant center during the intervening 9 yr between photographs. North is at top, east to the left.

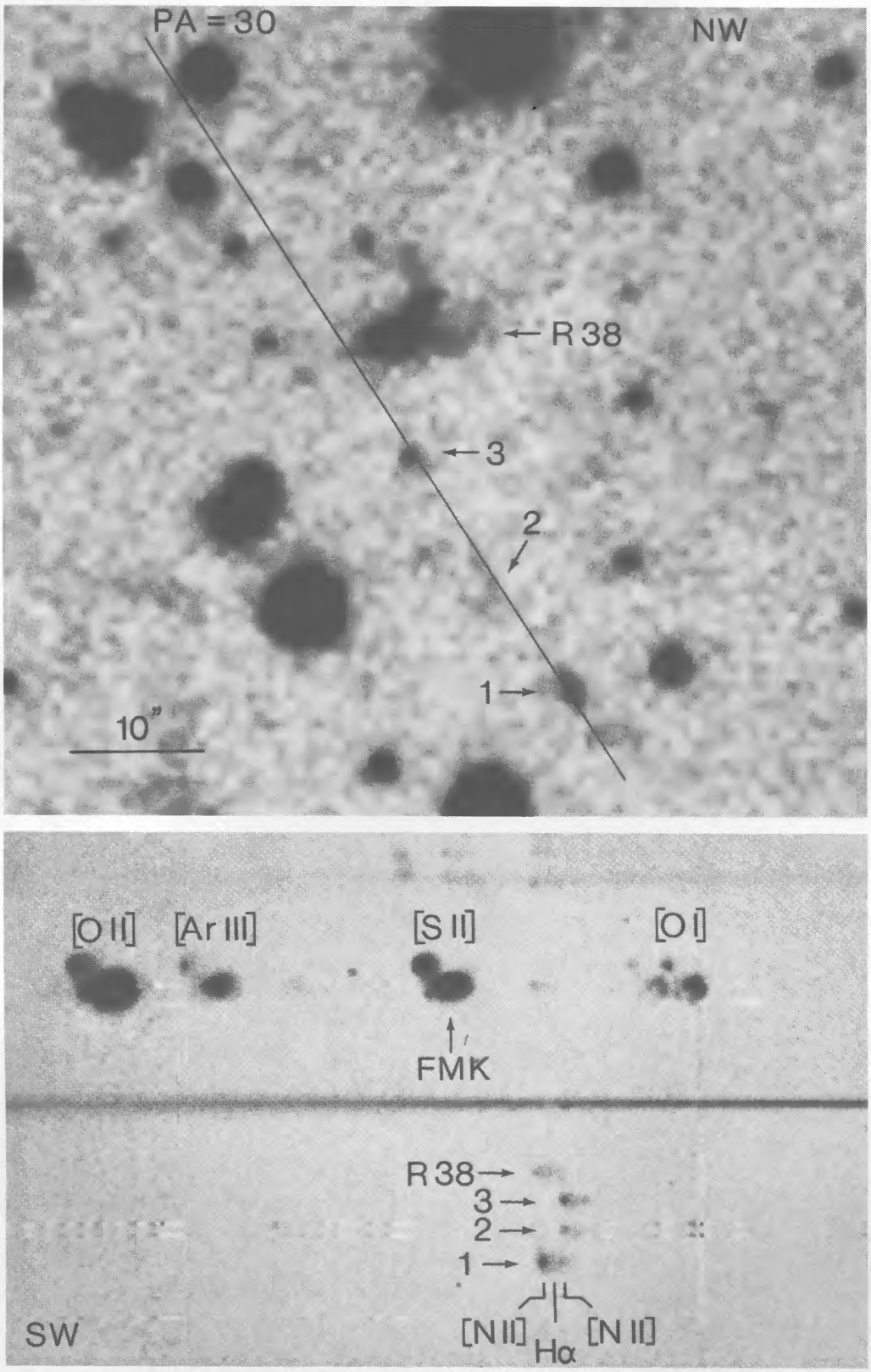


FIG. 4.—Slit position and spectra of south-southwest FMFs. (*top*) Positioning of lower half of slit, intercepting FMFs 1, 2, 3 and the faint diffuse outskirts of QSF R38. (*bottom*) Resulting spectrum covering the 6200–7400 Å spectral region (note: $\lambda$ decreases to the right), showing detection of only Hα and [N II] emission from the FMFs. Line identifications for a bright FMK (KB 40) intercepted along the remnant's southwestern rim are also shown for comparison.

south or outside these emission condensations. The spectra for features 1–3 (see Fig. 5) show an [N II]/Hα emission ratio near the high end of that observed for QSFs; specifically, 6583/Hα = 2.8–4.1, compared to a reported range for QSFs of 1.0–3.7 (Kirshner and Chevalier 1977). The next strongest observed line in QSFs is that of [O I] λ6300. At a 6300/Hα intensity ratio of 0.22 or less as seen in QSFs, any [O I] emission present would be below the detection limit of our spectrum. While relatively small radial velocities were found for knot 1 and R38 (−425 and −40 km s$^{-1}$ respectively), knots 2 and 3 showed much larger values, of −2150 and −2175 km s$^{-1}$. These are substantially greater than the 0 to −450 km s$^{-1}$ observed for QSFs (van den Bergh and Kamper 1983) but compatible with those seen for FMKs which lie at similar radial distances from remnant center, e.g., in the northeast jet.

A second image positioned ~70″ farther south was also obtained and is shown in Figure 6 (Plate 5). Small misalignments between the Hα + [N II] and continuum image produced somewhat of a three-dimensional effect for star images in the difference display, accentuating somewhat the emission structures detected. Whereas previously QSF R40 was just barely detected on the best published photographs, this feature is easily visible in this figure and is better placed within the frame than in our previous image. R40 can now be seen to show a distinct elongated appearance with approximate dimensions of 5″ × 10″. Considerable general diffuse emission is also present in this region as well but is limited to a fairly well defined area with a rather sharp western edge.[3] Because of this emission's location near R40 and its north-south alignment, it might be a continuation of the north-south line of QSFs and diffuse emission noted in the previous image. Other than the QSFs R39 and R40, there do not appear to be any other bright emission knots in this region.

Deep imaging of two fields located nearly due east of the remnant (see Fig. 1) were also obtained and are shown in Figure 7 (Plate 6). These images were taken in an effort to clarify the structure of a faint patch of emission present in this area. Very faint diffuse nebulosity in this region and in the immediate general vicinity of Cas A had been first noted by Minkowski (1968). This emission was interpreted as representing a very faint H II region which might be related to Cas A's suspected massive progenitor star. The best previous photographs of this eastern emission include Minkowski's original

[3] This diffuse emission may have been just barely detected on a deep red plate made by Minkowski in 1951; see photograph in van den Bergh (1971*a*).

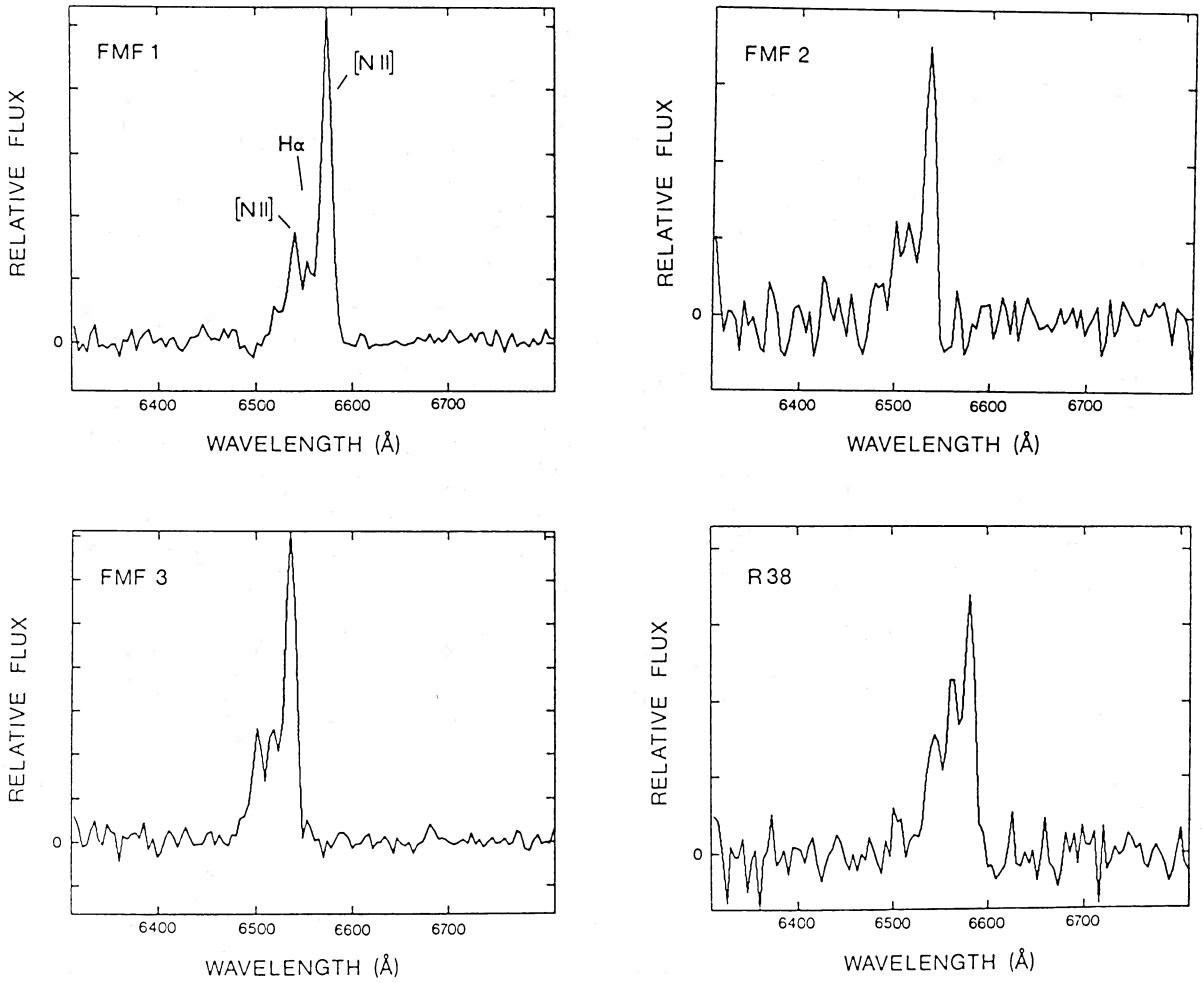


FIG. 5.—Spectra of the three FMFs and QSF R38 located south-southwest of the remnant. Relative flux vs. observed wavelength for the Hα + [N II] spectral region is shown.

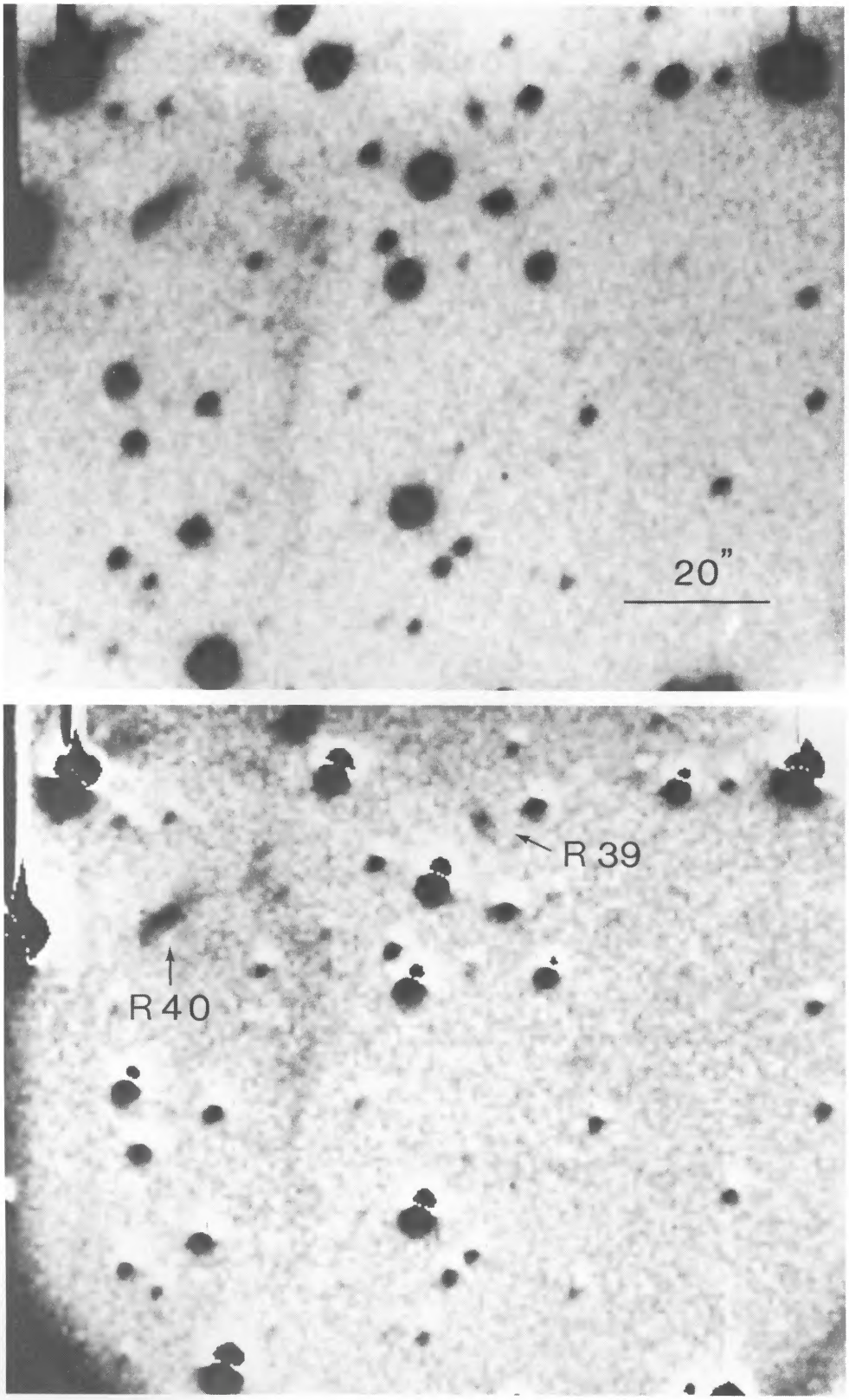


FIG. 6.—(*top*) Deep CCD image of the region further to the south from Fig. 4. (*bottom*) Image with red continuum frame partially subtracted to enhance emission features.

FESEN, BECKER, AND BLAIR (*see* page 382)

PLATE 6

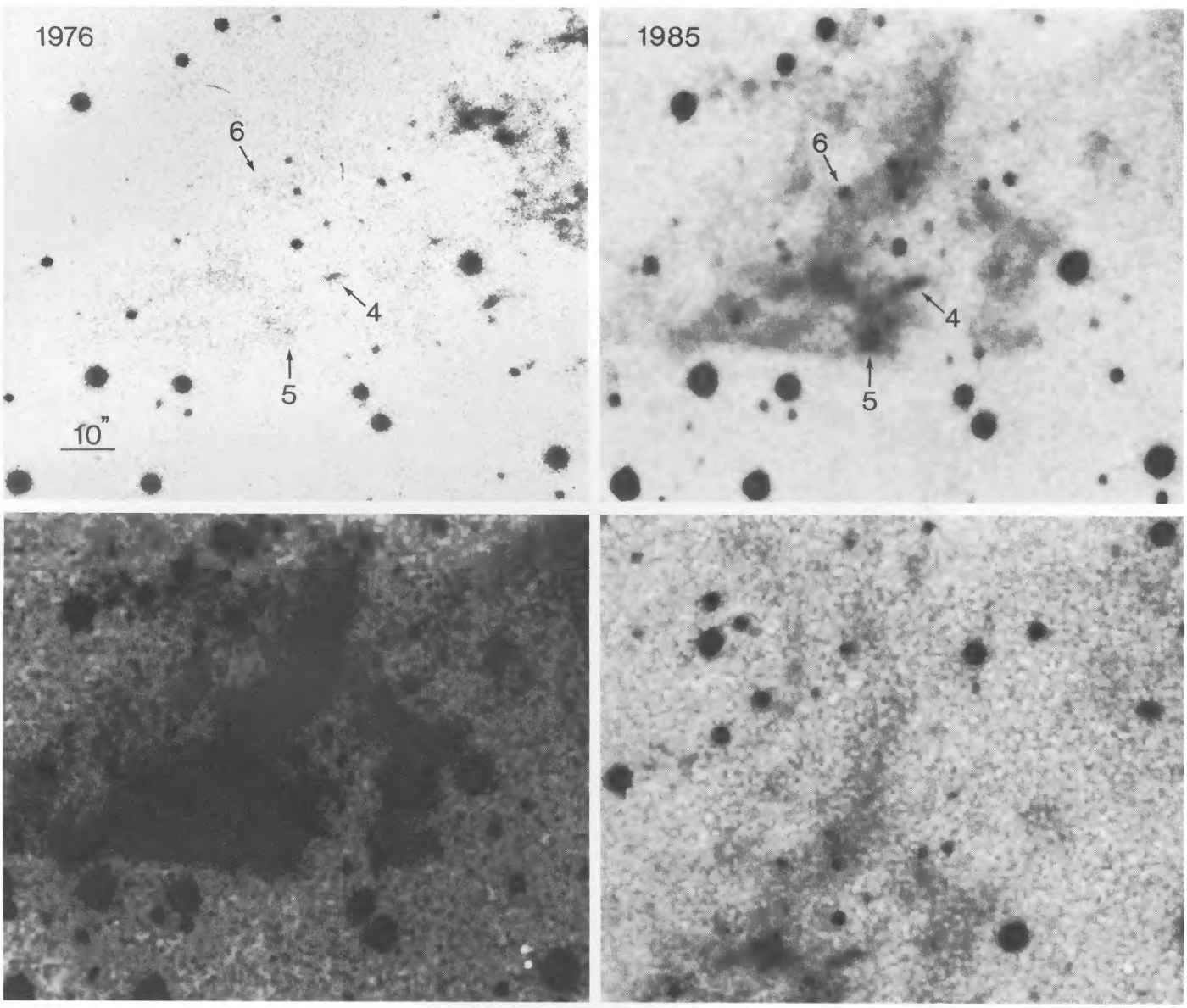


FIG. 7.—Area east of the remnant's main shell. (*top left*) Enlargement of the 1976 5 m plate with three suspected emission knots associated with the remnant indicated. (*top right*) 1985 CCD image taken using an Hα + [N II] narrow-passband interference filter of the same area and shown to the same scale. Note the presence of considerable diffuse emission in the region as well as the substantial angular displacements of knots 4, 5, and 6 compared to the 1976 image. (*bottom left*) High-contrast print of CCD image showing maximum detected extent of the diffuse nebulosity. (*bottom right*) Short (150 s) CCD exposure of the diffuse emission's structure centered 30″ further north.

FESEN, BECKER, AND BLAIR (*see* page 382)

plate (see van den Bergh 1971*a*) and a 1976 5 m plate taken by van den Bergh and Kamper (1983). Both of these showed only a diffuse and somewhat structureless patch of emission. An enlargement of this latter photograph is reproduced in Figure 7 for the same region and to the same scale as our CCD image. (The bright emissions to the upper right on the 1976 broad passband image are due to FMKs located along the remnant's eastern shell rim for which our interference-filter image is insensitive.) Our CCD image reveals significantly fainter emission which appears to have a fairly well defined structure. Most noticeable is a largely diffuse and triangular-shaped emission structure with an ill-defined eastern border and a fainter emission region to its west. Its "wispy" northernmost filaments appear to gradually curve to the east, suggesting an association with the jet's FMKs. This emission also exhibits a very sharp southern boundary, below which no emission was detected on either on our direct images or spectra (see below). A prominent south-central knotlike feature $\sim 3$ times brighter than neighboring diffuse emission along with three other fainter knots (Nos. 4, 5, and 6) were also detected in this region. Finally, a faint, curious 4″ diameter ringlike feature located just a few arcseconds north of feature 5 appears to be real, but its nature is unknown.

A comparison of our 1985 image to the 1976 photograph revealed that three knots (Nos. 4, 5, and 6) exhibited large proper motions ($\mu = 0\farcs5 \pm 0\farcs1$ yr$^{-1}$) during that time interval (see Table 1). While feature 6 appears just marginally detected in the 1976 photograph, features 4 and 5 stand out quite clearly and show a definite displacement. Because of the use of a narrow H$\alpha$ + [N II] interference filter, these knots are unlikely to be oxygen and sulfur emission FMKs but instead are probably similar to the high proper motion "QSF–like" emissions found in the south-southwest. All three knots exhibit substantial motions to the east and away from the remnant's center of expansion as given by Kamper and van den Bergh (1976). Moreover, feature 5 turns out to be visible on a 1958 image (see van den Bergh and Dodd 1970), confirming its rapid motion as well as permitting an improved estimate of its proper motion. Its presence on this early photograph also implies an optical emission lifetime of at least 27 years.

A spectrum of the extended diffuse nebulosity east of Cas A was subsequently obtained using the KPNO 4 m CCD spectrograph, with the resultant spectrum shown in Figure 8. A $3\farcs2 \times 4\farcm5$ slit was placed so as to sample as large a portion of the emission as possible, including the brightest knot (feature 7). Only the lower portion of the slit's length is shown in Figure 8, with the slit's upper portion extending further north across the base of the northeastern jet and filaments. Consequently, spectra of several FMKs were serendipitously obtained. A few exceedingly faint FMKs situated near the diffuse nebula's northern extreme were detected and show strong [S II] line emission and radial velocities up to $-4400$ km s$^{-1}$. Much brighter emission was detected from an FMK located just north of these and just east of FMK KB 105. The spectrum of the bright extended knot 7 and its surrounding diffuse emission is shown in Figure 9. Measured relative line intensities are listed in Table 2. Strong lines of [N II] and [S II] can be seen along with much weaker [O II], [O III], and [Fe II] emission relative to the strength of H$\alpha$. Due to the relatively low spectral resolution of 15 Å, the [S II] doublet was not resolved, thus preventing an estimate of the electron density. We did not find significant line intensity differences for this knot compared to that seen for the general diffuse nebulosity. However, within this feature, there is high-velocity [N II] emission as illustrated in Figure 8. As no high-velocity [S II] emission was detected, this suggests that it is not just a part of the diffuse nebula, but instead, is spectroscopically similar to QSFs, showing strong [N II] line emission. Its measured radial velocity of +400 km s$^{-1}$, however, would make it the most positive radial velocity QSF known. In view of the presence of three apparent "fast-moving QSF–like" features in the area, as well as its position well outside of the remnant's shell, it seems more likely to be another one of these. Thus, there appear to be three definite and one probable high-velocity "QSF–like" features in this region east of the remnant similar to the three found in the south-southwest.

## IV. DISCUSSION

Our CCD images have revealed the presence of very faint and extended diffuse emission plus several new emission knots located outside to the east and southwest of Cas A's main emission shell. Proper motions and spectroscopy for a few of these outlying emission knots indicate the existence of a previously undetected type of optical emission associated with the remnant. The three emission features to the southwest are perhaps the clearest examples of this type of emission. They exhibit H$\alpha$ and [N II] emission like that of QSFs yet also show large proper motions and radial velocities like the FMKs. This new type of emission does not appear to be confined to just this small southwest region. Proper motion estimates and detection on narrow H$\alpha$ + [N II] filter images suggest the presence of three other similar knots (and possibly a fourth from spectral data) located along the remnant's eastern edge. Because these knots combine the spectroscopic properties exhibited by the quasi-stationary flocculi with the kinematics of the fast-moving knots, we call them "fast-moving flocculi" (FMFs).

Due to their large proper motions and in some cases also large radial velocities, FMFs appear to be ejecta directly from the supernova outburst. With the exception of the FMKs in the northeast jet, they in fact comprise the remnant's highest velocity material; i.e., the FMKs in the main shell show space velocities as high as 6000 km s$^{-1}$ (van den Bergh 1971*b*; Kamper and van den Bergh 1976), compared to FMFs which have velocities in the range 6500–8500 km s$^{-1}$. Because the surface layers of the progenitor star are expected to experience the largest accelerations and subsequently show the highest velocities, the observation that FMFs possess the largest velocities implies that they probably represent fragments from near the star's photosphere at the moment of the SN explosion. We show below that FMFs consequently provide valuable insights for understanding some properties of the remnant and of the Cas A progenitor star.

Despite the somewhat limited spectral and positional data on FMFs, some statements can be made concerning their elemental abundances and kinematic properties. Although only a few line emissions are observed, it seems likely that FMFs are nitrogen-rich relative to cosmic N/H values. Since FMFs have QSF–like spectra with similar [N II]/H$\alpha$ ratios, previous abundance analyses yielding nitrogen overabundances of about a factor of 10 or more for QSFs (Peimbert and van den Bergh 1971; Chevalier and Kirshner 1978) might also apply as well to FMFs. Large [N II]/H$\alpha$ ratios are usually indicative of appreciable nitrogen enrichment like that found in QSFs as well as several other supernova remnants (e.g., Puppis A and Kepler's SNR). Thus, the relatively large [N II]/H$\alpha$ ratios observed for FMFs equal to or greater than those reported for QSFs might

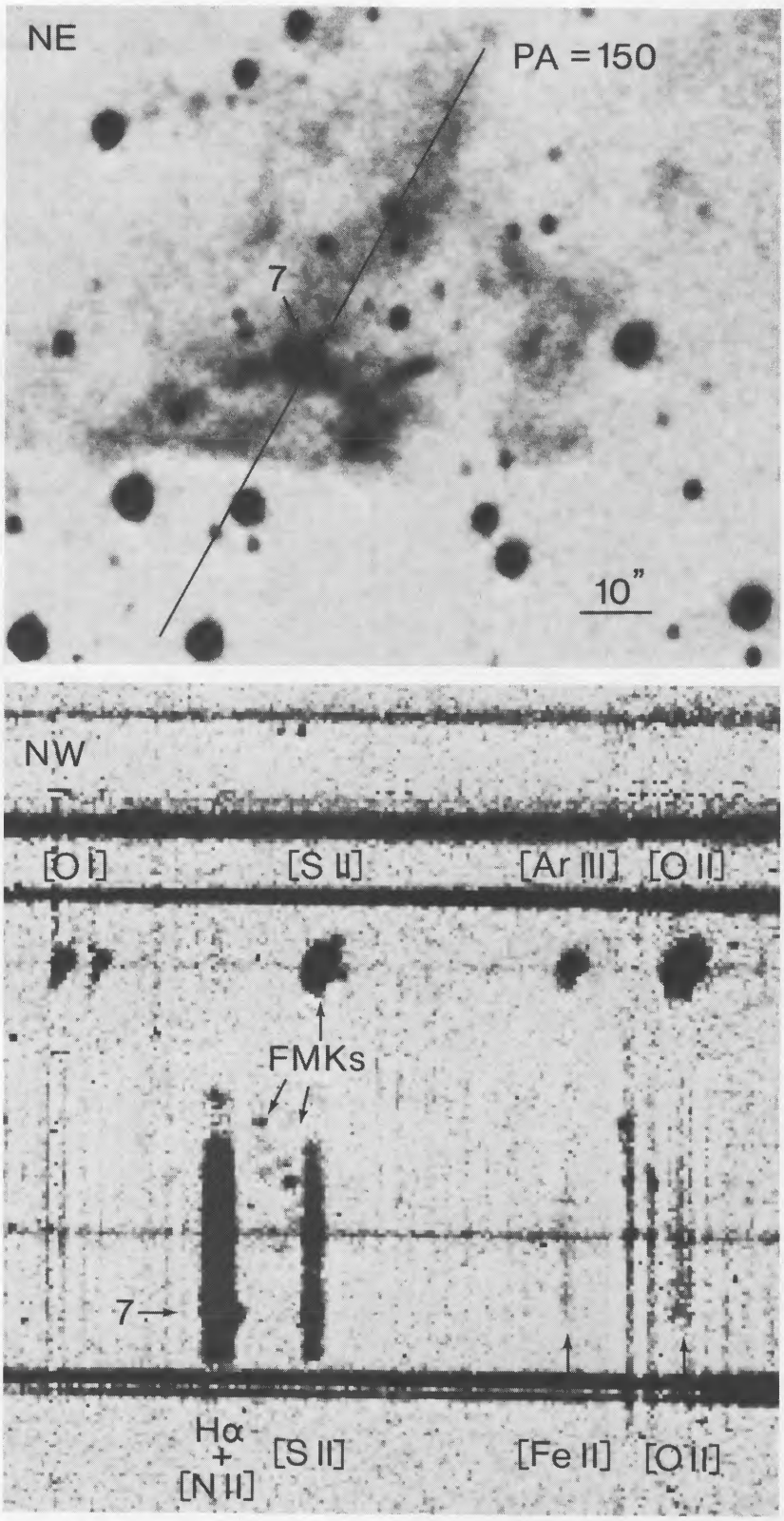


FIG. 8.—Slit position and spectra of emission east of Cas A. (*top*) Position of the lower half of the slit on diffuse nebula and bright knot No. 7. (*bottom*) Resulting 3000 s spectrum covering the region 6300–7400 Å for the entire slit length. The bright FMK shown in the spectrum is located near the base of the remnant's northeastern jet and is not within the area shown in the upper panel. Spectrum of knot 7 indicates the presence of high-velocity [N II] but with no detected high-velocity [S II] emission.

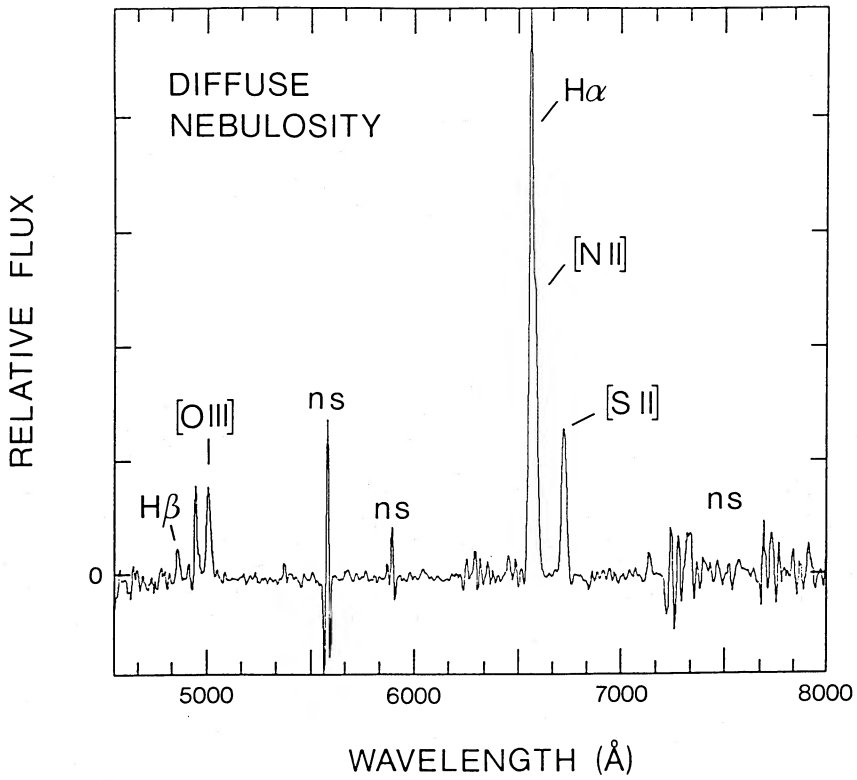


FIG. 9.—Spectrum of the extended diffuse nebulosity located just east of Cas A; relative flux vs. observed wavelength. Apparent features at 5577 Å, 6300 Å, and near 7200 Å are due to imperfect subtraction of airglow emission. Note that the relative intensity of the [O III] λ4959 line as shown is incorrect due to a coincident radiation "hit."

also imply by analogy a similarly large nitrogen overabundance for the FMFs. Moreover, since FMFs are supernova ejecta, their electron densities are likely to be at least as high as the $10^3$–$10^4$ cm$^{-3}$ estimated for the circumstellar QSFs (Chevalier and Kirshner 1978). Densities greater than $10^4$ would weaken the [N II] nebular lines due to collisional deexcitation, thereby leading to an underestimate of the nitrogen abundance using line intensities alone. Therefore, the observed strength of [N II] relative to Hα in FMFs suggests a nitrogen enrichment similar to or possibly larger than the $N/H \geq 10 \times (N/H)_{solar}$ estimated for the QSFs. An investigation into their helium abundance, the other element which appears overabundant in QSFs, unfortunately, may prove difficult. The intrinsic faintness of the FMFs identified here as well as the expected weakness of the He I λ5876 line if similar in strength to that seen in QSFs [i.e., $0.2 \times I(\mathrm{H}\alpha)$] will make accurate measurements of an FMF's helium line emission rather difficult to obtain.

While possessing large space velocities like FMKs, the FMFs we have discovered are positionally and kinematically distinct from the bulk of the remnant's other high-velocity emission knots. Whereas most of Cas A's FMKs lie at radial distances of 2′ or less and have radial proper motions between 0.″2 and 0.″5 yr$^{-1}$, FMFs exhibit proper motions in excess of 0.″5 yr$^{-1}$ and consequently lie outside the 2′ main shell radius. In this respect, they resemble more closely the FMKs found in the northeastern jet. However, the fact that FMF radial distances are less than those seen for some of the heavy element–rich jet knots implies that some core material was ejected to even higher velocities than that of the surface of the original star. This apparent "fountain-like" ejection of core material visible in the jet indicates at least a partially asymmetric supernova explosion. This has long been suspected due to the presence of the jet but unconfirmed until now due to uncertainties regarding the progenitor's surface composition and true remnant dimensions. There is additional evidence for an asymmetric stellar disruption in Cas A including: (1) asymmetrical Doppler shifts of X-ray line emission (Markert *et al.* 1983), (2) a ~2000 km s$^{-1}$ velocity difference between red- and blue-shifted main shell FMKs (Minkowski 1968; Braun 1985), and (3) the location of the highest observed radial velocity FMK projected some 75″ away from the remnant's center of expansion (van den Bergh 1971*b*). Although the actual global structure implied for the remnant by these observations is not yet clear, what is clear is that the star did not experience a completely uniform explosive expansion.

The detection of FMFs in both the two outlying regions we observed suggests that the FMFs we have discovered may represent only a fraction of the total number associated with the remnant. Indeed, an examination of published long-exposure photographs of Cas A (e.g., Kamper and van den Bergh 1976; van den Bergh and Kamper 1983, 1985) indicates the probable existence of two more FMFs located northwest of the remnant's expansion center as well as a possible one to the southeast (see Fig. 10 [Pl. 7]). These features are visible on broad-band red plates but not on [S II] or [O III] plates and appear to have proper motions and radial distances comparable to the FMFs in the east and southwest regions (see Table 1). However, additional detections of such features in other outlying regions might be hampered by strong extinction variations across the region, especially west of the remnant (Troland, Crutcher, and Heiles 1985). Moreover, the coin-

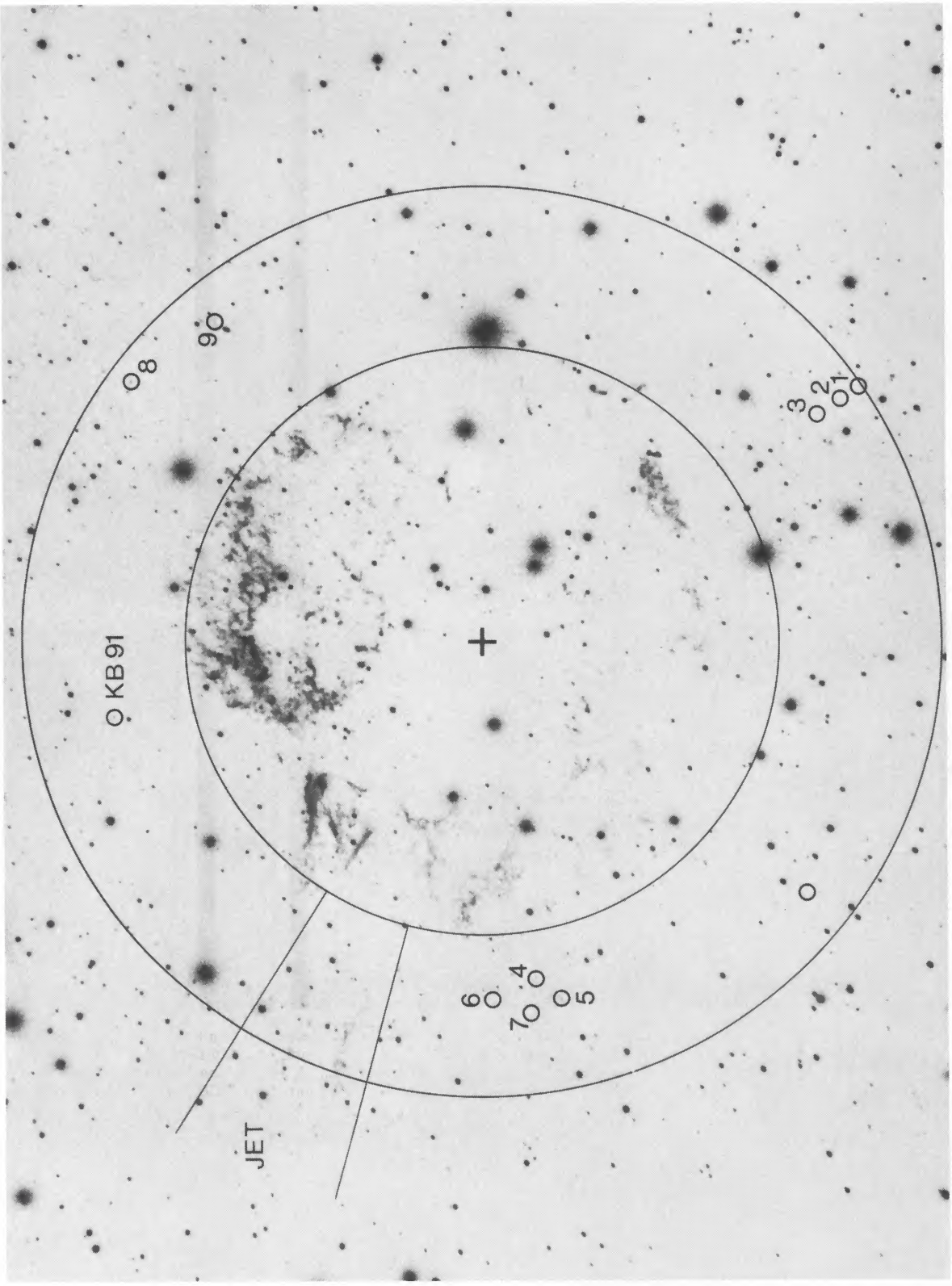


FIG. 10.—Reproduction of van den Bergh and Kamper's (1985) deep 1983 broad-band red photograph of Cas A. The plus marks the remnant's center of expansion, with the inner circle (radius = 127") indicating the approximate angular dimension of the remnant's main shell. The larger circle (radius = 196") indicates the outer boundary of the remnant's outlying optical emission knots. These emission features include the fast-moving knot KB 91 to the north, the FMFs Nos. 1–3 to the southwest, the FMFs 4–7 to the east, the probable FMFs 8 and 9 to the northwest, and a possible FMF to the southeast.

cidence of FMFs 1–7 with regions having appreciable diffuse emission suggests their excitation (and hence their visibility) is due to their interaction with the denser interstellar medium. The optical line emission of FMFs probably results from their high-speed passage through the interstellar gas driving a slow reverse shock into the knot. This would make it appear to "light up" due to radiative recombination losses in the post-shock cooling zone. Thus, the visibility of the southwest FMFs would be due to the QSFs and associated material located in this region (e.g., R36–R38, and R40), as well as the diffuse emission present there. Likewise, the diffuse nebulosity east of the remnant would be responsible for the optical detection of the northeast jet and FMFs found in this region. Sufficiently high knot densities producing rapid cooling [$\tau \approx (\alpha_{\rm rec} n_e)^{-1}$] or clumpiness of the local interstellar medium or both could account for the rapid brightness changes in FMFs such as the fading of FMF 1 (=R39) from 1976 to 1983. An electron density of $\sim 10^4$ cm$^{-3}$ for FMF 1 would then be required.

The extended diffuse emission to the east and southwest of the remnant could either be a part of the local H II region with which the Cas A progenitor star had been once associated (Minkowski 1968; Peimbert and van den Bergh 1971) or instead represent mass lost by the star prior to its QSF mass loss episode. Its spectrum certainly suggests a less nitrogen-rich gas than that of the QSFs and FMFs. Although its H$\alpha$/[S II] ratio of 2.2 is near the maximum seen for shock-heated remnant gas and much smaller than is typically seen for H II regions, it is not unlike that observed for some low-ionization photoionized nebulae (Blair, Kirshner, and Chevalier 1981). Due to the apparent lack of nearby OB stars, Peimbert (1971) and van den Bergh (1971*a*) suggested that this and other local nebulosities might be excited by the UV and X-ray emission of the SN outburst, since densities below 100 cm$^{-3}$ would produce a recombination time scale greater than $10^3$ yr. Regardless of its source of excitation, however, its peculiar structure probably reflects its direct contact with the Cas A remnant as well as its close proximity to the presupernova star. Part of this nebulosity might represent stellar mass loss material from the progenitor star, and Chevalier and Kirshner (1978) have speculated that some early mass loss material might remain in the immediate area of the presupernova star.

If the FMFs detected to the east and southwest of the remnant (and suspected in the northwest and southeast) are indicative of a remnant-wide phenomenon, as Figure 10 suggests, then their radial distances of 2.'4–3.'2 suggest a somewhat larger optical remnant than was previously realized but one still consistent with observations of Cas A at radio and X-ray wavelengths. Weak radio emission has been detected outside the main radio shell to the north, east, and southwest out to distances of 2.'5 (Bell's knots 24, 34, and 38), although there does not seem to be coincident radio emission with either the FMFs or outlying diffuse nebulosity. However, in X-rays the remnant shows both a 100″ radius bright main shell and a much fainter outer "plateau" to the north and south out to a radius of ~140″ (Fabian *et al.* 1980). This is nearly the radial distance observed for the FMFs in the east but ~35″ less than that for the FMFs in the southwest.[4] Since FMFs are probably ejecta from the surface of the progenitor star, they should lie close to or possibly just slightly ahead of the remnant's main blast wave. This would then imply a mean blast wave velocity of 6500–7500 km s$^{-1}$, which is consistent with the X-ray data (Markert *et al.* 1983). Therefore, the observed X-ray plateau between 100″ and 140″ may signify a reverse shock emission zone of interstellar gas behind the FMFs. As the bulk of the remnant's ejecta encounters this high-temperature and high-pressure reverse shock region, rapid heating of the lower density ejecta results in increased soft X-ray emission (Markert *et al.* 1983), with optical emission produced from the denser knots (see Dopita, Binette, and Tuohy 1984). Ejecta with velocities of less than 4000 km s$^{-1}$ might not yet have reached the high-pressure reverse shock region and thus would not be optically visible, consistent with the observations (van den Bergh 1971*b*; Chevalier 1981).

This picture, in which the FMFs together with the FMKs in the northeast jet lie in front of the remnant's blast wave, may also explain differences in estimates for the age of the remnant. FMF radial distances and proper motions imply an explosion date $T_0$ more in line with the A.D. 1671 value deduced from the jet's FMKs than the A.D. 1653 date derived using only FMKs located in remnant's main shell (see Table 1). The apparent agreement in extrapolated dates for the supernova outburst using the remnant's highest velocity ejecta—i.e., the heavy element–enriched FMKs in the jet and the nitrogen-rich FMFs—is unlikely to be a coincidence. Rather, it is probably due to less deceleration compared to that experienced by the main shell's reverse shock-heated ejecta and thus should yield a more accurate date for the explosion. However, even the fast-moving outlying material should have undergone some deceleration. If one adopts a derived date of around A.D. 1670 and assumes a small amount of deceleration (~3% over 300 yr) for the FMFs and the FMKs in the jet via interaction with the surrounding medium (necessary to provide the reverse shock excitation for their optical visibility), then arguments in support of the possible Flamsteed sighting of the actual supernova outburst in 1680 August appear more plausible (Ashworth 1980; Brecher and Wasserman 1980). The near coincidence of derived and reported dates, the position of Flamsteed's "star" 3 Cas relatively close to Cas A's location, and Flamsteed's otherwise small misidentification percentage, while not conclusive (cf. Broughton 1979; Kamper 1980), are certainly suggestive that he serendipitously observed the Cas A supernova.

Perhaps the most important aspect of the discovery of fast-moving nitrogen-rich emission is what it implies about Cas A's progenitor star. The fact that FMFs possess space velocities greater than the bulk of Cas A's FMKs implies they probably are fragments from near the star's photosphere at the moment of supernova outburst. This, together with the spectral similarity between FMFs and QSFs, suggests that the star's hydrogen- and nitrogen-rich envelope had not been completely removed prior to the supernova event, as had been previously believed (Chevalier 1976; Chevalier and Kirshner 1978). The presence of some remaining envelope material resolves an apparent inconsistency regarding Cas A. The remnant's FMK abundances suggest a massive Type II SN event but because of its apparent faintness was thought to involve a small-radius star whose hydrogen-rich envelope was completely removed prior to the explosion (Chevalier 1976). Since FMFs seem to contain substantial hydrogen, Cas A's supernova should have exhibited strong hydrogen emission and thereby would have fulfilled the spectroscopic criteria of Type II SN identification.

[4] A 6′ radius X-ray halo surrounding the remnant (Stewart, Fabian, and Seward 1983) may not be real but rather a combination of instrumental and dust scatterings effects (Mauche 1984; Mauche and Gorenstein 1985).

Moreover, the observed difference in ejected velocities between FMF 1 and FMF 3 (i.e., 7400 and 8600 km $s^{-1}$) may suggest a fairly substantial envelope still attached to the star at time of outburst.

There are now several indications that seem to point to a massive Wolf-Rayet stellar progenitor. Evidence for appreciable stellar mass loss prior to the explosion (Peimbert and van den Bergh 1971; Chevalier and Kirshner 1978) together with the presence of Si-group element enrichment in the FMKs, indicating the occurrence of oxygen burning and thus implying a lower mass limit of 9 $M_\odot$ (Arnett 1975; Lamb 1978), have long suggested a massive, early-type star. Furthermore, studies of the remnant's X-ray emission estimate a remnant mass of 15 $M_\odot$ or more (Fabian *et al.* 1980; Markert *et al.* 1983). Although this value is somewhat uncertain, it does suggest a large initial mass ($\sim$40 $M_\odot$ or more) for the progenitor star. The minimum initial stellar mass necessary for forming W-R stars is currently thought to be around 20 $M_\odot$ but with the majority of W-R stars originating from stars having masses greater than 40 $M_\odot$ (Firmani 1982; Schild and Maeder 1984). If the surface composition was as nitrogen-rich as our FMF spectra suggest (N/H $\geq$ 10 that of solar), then a WN progenitor star is indicated. Nitrogen overabundance in red giants is much lower, being only 3–4 times over cosmic values (Luck 1978). For the most massive stars, CNO processing enrichment can quickly increase the $^{14}$N surface abundance by a factor of $\sim$6 via $^{12}$C destruction, but larger values are possible via $^{16}$O destruction leading to a twelvefold increase in $^{14}$N (Maeder 1983). Large N/H values, like those seen in W-R stars, are then both the result of this N enrichment together with substantial hydrogen-rich envelope mass loss. The Wolf-Rayet subtypes WC and WO can be definitely excluded as progenitor candidates, since these stars have little if any hydrogen and are also underabundant in nitrogen. While connections between the mass loss undergone by Cas A's progenitor and that seen in Wolf-Rayet and similar early-type stars have been previously proposed (e.g., Walborn 1976; Chevalier 1976, 1981), our observations indicating a nitrogen-rich envelope for the star at the time of supernova outburst provides direct evidence for a WN-type spectroscopic classification.

A large initial mass, substantial mass loss, and a hydrogen- and nitrogen-rich photosphere in fact specifically suggest a late WN (i.e., WN7–WN9) progenitor star for Cas A. These stars rank among the most massive W-R stars, having estimated masses in the range of 60 $M_\odot$ or more (Schild and Maeder 1984) and thus would satisfy the large remnant X-ray mass estimates. Although these stars have probably just started their W-R phase and have not been previously viewed as good SN candidates (Maeder and Lequeux 1982; Doom, De Greve, and De Loore 1986), they are the only type of W-R star to have sufficient hydrogen-rich envelopes to explain the properties of the FMFs; i.e., $N(\mathrm{H})/N(\mathrm{He}) > 0.8$ (Conti, Leep, and Perry 1983). The hydrogen observed in FMFs is an important constraint for potential progenitor star candidates, since it cannot be attributed to swept-up material. This would require an accreted hydrogen mass several times that contained in the original knot. Furthermore, late-type WN stars also have model predicted N/He ratios of $\sim$0.01 (Maeder 1983) and observed values of 0.007–0.04 (Willis 1982) consistent with a nitrogen overabundance of 10 or greater, like that suspected in the FMFs.

Interestingly, late-type WN stars and in particular WN8 stars also seem to exhibit the nitrogen-rich, low-velocity and high-density mass loss nebula thought necessary to produce Cas A's nitrogen-rich QSFs. Of all the W-R stars exhibiting associated optical nebula, only two, both associated with WN8 stars, are believed the result of high-density, low-velocity mass ejections. These two nebulae, M1–67 associated with the star 209 BAC, and RCW 58 surrounding the star HD 96548, appear to consist of clumpy and nitrogen-rich material ejected from the central W-R star (Chu, Treffers, and Kwitter 1983). The 209 BAC/M1–67 star/ring nebula system appears especially interesting as a possible Cas A progenitor case. The nebula M1–67 has high electron densities ($\sim 10^3$), a low expansion velocity (42 km $s^{-1}$), and an age of $\sim 10^4$ yr similar to the inferred properties for Cas A's QSFs (Kamper and van den Bergh 1976; Chevalier and Kirshner 1978; Solf and Carsenty 1982). M1–67 also has a relatively high space velocity of 220 km $s^{-1}$, and such a large space velocity progenitor + ring nebula could explain the asymmetry observed in the QSF's radial velocities (i.e., $V_r = 0$ to $-450$ km $s^{-1}$). Curiously, no WN8 star has yet been found in an open cluster. Similarly, no early-type stars have been found near Cas A (van den Bergh 1971*a*), although at an estimated distance of 2.8 kpc it has usually been presumed connected with the Cas OB2 association lying at a distance of 2.63 kpc (Humphreys 1978). Since a majority of WN8 stars are suspected as having low-mass, compact binary companions, in contrast to the OB companions frequently seen for WN7 stars, they may thus represent "runway" systems (Lundstrom and Stenholm 1984). If Cas A's progenitor was a WN8 star, this might also resolve the lack of nearby OB stars despite its inferred large initial mass. Finally, the recent observation of an extragalactic Type II SN showing indications of a W-R spectrum at early times, and specifically, strong N III emission indicative of a late WN classification (Niemela, Ruiz, and Phillips 1985), shows that in at least some Type II SNs, late-type WN stars appear to be involved. Therefore, while we conclude that Cas A no longer appears to be the disruption of a WO star, as earlier suspected and recently argued by Filippenko and Sargent (1986) and Begelman and Sarazin (1986), we caution, however, that it is not at all clear that all oxygen-rich supernova remnants represent the final stage of WN evolution.

It is a pleasure to thank R. Kirshner and P. F. Winkler for obtaining the 4 m spectrum of the southwest FMFs for us, S. Voels for assistance in its final reduction, M. Shull for encouragement and support, and to P. Conti, A. Hamilton, R. Kirshner, H. Itoh, C. Mauche, C. Sarazin, F. Seward, and L. Smith for useful discussions and correspondence. We are also grateful to S. van den Bergh for providing film copies of his 1976 5 m plate of Cas A and wish to acknowledge the valuable observing and data reduction assistance of both the KPNO and Lick Observatory staffs and in particular J. Barnes, R. Goodrich, and R. Stone. This research was partially funded by NSF grants AST 82-16481 and AST 84-19370 and by grants from the University of Colorado and The Johns Hopkins University's Center for Astrophysical Sciences.

REFERENCES


Arnett, W. D. 1975, *Ap. J.*, **195**, 727.
Ashworth, W. B. 1980, *J. Hist. Astr.*, **11**, 1.
Baade, W., and Minkowski, R. 1954, *Ap. J.*, **119**, 206.
Begelman, M. C., and Sarazin, C. L. 1986, *Ap. J. (Letters)*, **302**, L59.
Bell, A. R. 1977, *M.N.R.A.S.*, **179**, 573.
Blair, W. P., Kirshner, R. P., and Chevalier, R. A. 1981, *Ap. J.*, **247**, 879.
Braun, R. 1985, Ph.D. thesis, University of Leiden.
Brecher, K., and Wasserman, I. 1980, *Ap. J. (Letters)*, **240**, L105.
Broughton, R. P. 1979, *J.R.A.S. Canada*, **73**, 381.
Chevalier, R. A. 1976, *Ap. J.*, **208**, 828.
———. 1979, *Ap. J.*, **233**, 154.
———. 1981, in *Supernovae: A Survey of Current Research*, ed. M. Rees and R. Stoneham (Dordrecht: Reidel), p. 419.
Chevalier, R. A., and Kirshner, R. P. 1978, *Ap. J.*, **219**, 931.
———. 1979, *Ap. J.*, **233**, 154.
Chu, Y.-H., Treffers, R. R., and Kwitter, K. B. 1983, *Ap. J. Suppl.*, **53**, 937.
Conti, P. S., Leep, E. M., and Perry, D. N. 1983, *Ap. J.*, **268**, 228.
Doom, C., De Greve, J. P., and De Loore, C. 1986, *Ap. J.*, **303**, 136.
Dopita, M. A., Binette, L., and Tuohy, I. R. 1984, *Ap. J.*, **282**, 142.
Fabian, A. C., Willingale, R., Pye, J. P., Murray, S. S., and Fabbiano, G. 1980, *M.N.R.A.S.*, **193**, 175.
Filippenko, A. V., and Sargent, W. L. W. 1986, *A.J.*, **91**, 691.
Firmani, C. 1982, in *IAU Symposium 99, Wolf-Rayet Stars: Observations, Physics, Evolution*, ed. C. W. H. DeLoore and A. J. Willis (Dordrecht: Reidel), p. 499.
Humphreys, R. M. 1978, *Ap. J. Suppl.*, **38**, 309.
Kamper, K. W. 1980, *Observatory*, **100**, 3.
Kamper, K., and van den Bergh, S. 1976, *Ap. J. Suppl.*, **32**, 351.
Kirshner, R. P., and Chevalier, R. A. 1977, *Ap. J.*, **218**, 142.
Lamb, S. A. 1978, *Ap. J.*, **220**, 186.
Luck, R. E. 1978, *Ap. J.*, **219**, 148.
Lundstrom, L., and Stenholm, B. 1984, *Astr. Ap. Suppl.*, **58**, 163.
Maeder, A. 1983, *Astr. Ap.*, **120**, 113.
Maeder, A., and Lequeux, J. 1982, *Astr. Ap.*, **114**, 409.
Mauche, C. W. 1984, *Bull. AAS*, **16**, 926.
Mauche, C. W., and Gorenstein, P. 1985, in *The Crab Nebula and Related Supernova Remnants*, ed. M. C. Kafatos and R. B. C. Henry (Cambridge: Cambridge University Press), p. 81.
Markert, T. H., Canizares, C. R., Clark, G. W., and Winkler, P. F. 1983, *Ap. J.*, **268**, 134.
Miller, J. 1983, *Lick Obs. Internal Rept.*
Minkowski, R. 1957, in *IAU Symposium 4, Radio Astronomy*, ed. H. C. van de Hulst (Cambridge: Cambridge University Press), p. 114.
———. 1959, in *IAU Symposium 9, Paris Symposium on Radio Astronomy*, ed. R. N. Bracewell (Palo Alto: Stanford University Press), p. 315.
———. 1968, in *Stars and Stellar Systems*, Vol. 7, *Nebulae and Interstellar Matter*, ed. B. M. Middlehurst and L. H. Aller (Chicago: University of Chicago Press), p. 623.
Niemela, V. S., Ruiz, M. T., and Phillips, M. M. 1985, *Ap. J.*, **289**, 52.
Oke, J. B. 1974, *Ap. J. Suppl.*, **27**, 21.
Peimbert, M. 1971, *Ap. J.*, **170**, 261.
Peimbert, M., and van den Bergh, S. 1971, *Ap. J.*, **167**, 223.
Schild, H., and Maeder, A. 1984, *Astr. Ap.*, **136**, 237.
Searle, L. 1971, *Ap. J.*, **168**, 41.
Solf, J., and Carsenty, U. 1982, *Astr. Ap.*, **116**, 54.
Stewart, G. C., Fabian, A. C., and Seward, F. D. 1983, in *IAU Symposium 101, Supernova Remnants and Their X-Ray Emission*, ed. J. Danziger and P. Gorenstein (Dordrecht: Reidel), p. 59.
Troland, T. H., Crutcher, R. M., and Heiles, C. 1985, *Ap. J.*, **298**, 808.
van den Bergh, S. 1971*a*, *Ap. J.*, **165**, 259.
———. 1971*b*, *Ap. J.*, **165**, 457.
van den Bergh, S., and Dodd, W. W. 1970, *Ap. J.*, **162**, 485.
van den Bergh, S., and Kamper, K. 1983, *Ap. J.*, **268**, 129.
———. 1985, *Ap. J.*, **293**, 537.
Walborn, N. R. 1976, *Ap. J. (Letters)*, **204**, L17.
Willis, A. J. 1982, in *IAU Symposium 99, Wolf-Rayet Stars: Observations, Physics, Evolution*, ed. C. W. H. De Loore and A. J. Willis (Dordrecht: Reidel), p. 87.


*Note added in proof 1986 October 27.*—Analysis of Cas A observations obtained in 1986 July using the Lick 3 m + CCD detector confirm the high proper motion of FMF 9 and indicate it to have $V_r = +1200$ km s$^{-1}$. A low-resolution spectrum of FMF 9 covering the range 4500–7200 Å showed only strong [N II] $\lambda\lambda$6548,6583 emission lines with no visible H$\alpha$ emission (i.e., [N II] 6583/H$\alpha$ > 20). This suggests that this knot originated from a deeper and more nitrogen-rich layer below the more H-rich surface layers responsible for FMFs 1–3. CCD images of the region around FMF 9 also revealed the appearance of a relatively bright knot $\sim$13″ northwest of FMF 9 which was not visible on 1983 photographs.


ROBERT H. BECKER: Physics Department, University of California, Davis, CA 95616

WILLIAM P. BLAIR: Department of Physics and Astronomy, Johns Hopkins University, 170 Rowland Hall, Baltimore, MD 21218

ROBERT A. FESEN: Center for Astrophysics and Space Astronomy, Campus Box 391, University of Colorado, Boulder, CO 80309